Improving Single Event Effects Testing Through Software

M. W. Banker, Jet Propulsion Laboratory, California Institute of Technology

***Abstract*-Radiation encountered in space environments can be damaging to microelectronics and potentially cause spacecraft failure. Single event effects (SEE) are a type of radiation effect that occur when an ion strikes a device. Single event gate rupture (SEGR) is a type of SEE that can cause failure in power transistors. Unlike other SEE rates in which a constant linear energy transfer (LET) can be used, SEGR rates sometimes require a non-uniform LET to be used to be accurate. A recent analysis shows that SEGR rates are most easily calculated when the environment is described as a stopping rate per unit volume for each ion species. Stopping rates in silicon for pertinent ions were calculated using the Stopping and Range of Ions in Matter (SRIM) software and CRÈME-MC software. A reference table was generated and can be used by others to calculate SEGR rates for a candidate device. Additionally, lasers can be used to simulate SEEs, providing more control and information at lower cost than heavy ion testing. The electron/hole pair generation rate from a laser pulse in a semiconductor can be related to the LET of an ion. MATLAB was used to generate a plot to easily make this comparison.**

***Index Terms*-SEGR, stopping rate, laser testing, generation equation**

I. Introduction

Space electronics have to be designed to withstand the radiation environments they will encounter. As transistors have shrunk in size with the advancement of technology, the effects of radiation on electronic parts have changed. Radiation professionals constantly strive to correctly emulate space radiation environments, test parts, and design devices that are radiation-hardened but affordable and functional [1]. The fly-by and orbiter proposed to be sent to Europa, one of Jupiter's moons, through the Europa Habitability Mission, would be put through Jupiter's extremely harsh radiation environments. Jupiter's magnetic field is ten times the magnitude of Earth's, and its radiation belts are a million times more intense than Earth's Van Allen belts. Ensuring the mission does not fail due to radiation would be one of the biggest challenges scientists and engineers must face. Radiation would affect every aspect of the mission, not only the functionality of the electronic parts but even the probability of Europa being habitable, for high-energy particles in jovian environments continuously hit Europa's surface ice, facilitating energy-producing reactions, and possibly providing enough energy to support life below the ice [2].

Radiation can affect parts through total ionizing dose (TID), displacement damage, and single event effects (SEE), among others. TID is the accumulated energy transferred to the oxide material of a transistor from all ionizing particles. Effects of TID in metal oxide semiconductor field effect transistors (MOSFETs) include threshold voltage shift, increased leakage current, and degradation of timing parameters. Microdose, a type of TID, occurs when a heavy ion strikes a very small structure in a device and causes significant degradation. [3] Displacement damage defects (DDD) are caused by the scattering of atoms in the semiconductor lattice with incident particles such as protons, neutrons, and high-energy electrons. These types of interactions are much more frequent than the hard collisions that cause SEE, and they occur in the bulk material of the transistor. Devices dependent on minority carriers are more susceptible to DDD, while MOSFETs are not. [3] Effects of DDD include leakage current, gain degradation, and reduced carrier mobility. [4] When a single particle causes a discernible effect in a device, a SEE occurs. Unlike TID, effects created by different particles are not added together to create an overall effect, but instead, only particles individually able to cause an event are pertinent to SEE. [3] There are many different types of SEEs, which can cause various effects such as transient current, bit upsets, and device failure, depending on the type.

II. Background

Single event gate rupture (SEGR) is a specific type of SEE that occurs when a heavy ion strikes the channel region of a power MOSFET, a primary element found on spacecrafts. SEGR is so important because it is a destructive event that can cause mission failure. As the ion travels through the power MOSFET's wide channel region, it deposits energy that generates electrons and holes. The electrons and holes cause the electric field in the oxide to increase, which in turn can cause oxide breakdown and device failure. Unlike other SEEs, the linear energy transfer (LET) of the ion cannot be considered a constant throughout the ion track as it travels through the device for some ion energies when calculating the SEE rate. Lower energy ions, which have higher LETs, lose significant amounts of energy as they travel through the power MOSFET's wide depletion region. These low energy ions are the highest contributors to SEGR rates. [5]

A recent analysis [5] shows that calculating the stopping rate per unit volume of each ion in silicon greatly simplifies the SEGR rate calculation. It's importance and derivation is outlined in [5]. Designated s_i for the ith

particle species, the stopping rate is a coefficient that describes the space radiation environment. The SEGR rate equation is given by

$$\sum_i s_i \int X_i(\tau) d\tau$$

where $X_i(\tau)$ is the directional-average SEGR cross section, which depends on the device. The equation shows how a reference table of the stopping rate for each ion in certain radiation environments can reduce the amount of work required to calculate the SEGR rate using the most recent and accurate method. [5]

Additionally, laser testing is another tool that aids in SEE testing. Typically, parts are irradiated with heavy ions to create SEEs, but a high-pulsed laser can also be used to induce SEEs in integrated circuits. Laser testing is an inexpensive, bench-top tool that provides greater control and more information that heavy ion testing allows. The laser can be pinpointed on a specific part of the integrated circuit, and the device's response can be monitored on a digital scope. This allows testers to know where precisely in the integrated circuit a single event effect is occurring, as well as see the device's response. While it cannot replace heavy ion testing, it is a supplement that can significantly reduce costs and further aid in ensuring parts are radiation-hardened. [6]

While laser testing and heavy ion testing are inherently different, their effect on a device is comparable. A laser pulse generates electron-hole pairs in a semiconductor, as does an ion strike, though the generation rates between the two cannot be directly compared. The laser generation rate can, though, be converted to a laser LET, which can be compared to a heavy ion's LET. The laser LET equation, derived from the laser generation equation, is a function of laser energy for certain device sensitivity depths. [6]

III. Objectives

The first objective was to create a reference table of the stopping rates per unit volume of ions hydrogen to uranium in silicon for four different radiation environments. The environments were 100 mils (2.54 mm) of aluminum shielding from spacecraft in interplanetary space during solar minimum and during solar flare, and 250 mils (6.35 mm) of aluminum shielding from spacecraft in interplanetary space during solar minimum and during solar flare. 100 mils of aluminum shielding was used because this is the default assumption used by radiation specialists when no other information is given, whereas 250 mils was used because this is a more realistic amount of shielding likely to be found on a spacecraft. The completed table will facilitate in calculating more precise SEGR rates.

The second objective was to create an easy to use plot in MATLAB of the equivalent laser LET versus laser energy for certain device sensitivities for the laser facility at the Jet Propulsion Laboratory. This will allow laser testers to quickly glance at the graph and know how to tune the laser to correctly emulate the desired LET.

IV. Methods

Stopping rate

Calculating the stopping rate per unit volume of each ion in silicon is a multi-step process that requires the use of two different software programs, the Stopping and Range of Ions in Matter (SRIM) [7] and Crème-MC [8], both available online.

The first step is to use SRIM to calculate the energy for each ion just able to penetrate 100 mils (2.54 mm) or 250 mils (6.35 mm), depending on the environment being used, of aluminum, $E_{T,i}$, where i is the atomic number of the element being used. The minimum and maximum energies need to be changed for each ion to include 2.54 mm (or 6.35 mm) in the chart produced by SRIM. In almost all cases, the energy for the desired amount of shielding must be extrapolated from the bordering energies, for 2.54 mm or 6.35 mm of shielding is rarely explicitly given in the table. For example, energies for 2.48 mm and 2.73 mm may be given by SRIM, and the energy for 2.54 mm must be extrapolated using a linear approximation. Then, SRIM is used again to calculate the LET, $L_i(E_{T,i})$, in the target material, silicon, for the energy of the ion found in the first step. Once again, the LET for the desired energy must likely be extrapolated from the given energies.

Crème-MC is a free software found online that describes radiation environments and aids in calculating SEE rates. For units consistency with the CRÈME-MC program, divide $E_{T,i}$ by the atomic mass unit (amu) for the particular ion to get $\frac{E_{T,i}}{m}$, measured in eV/nucleon. Then, find the omnidirectional differential flux, $h_{U,OMNI}(\frac{E_{T,i}}{m})$, for the ion species at energy $\frac{E_{T,i}}{m}$ using CRÈME-MC for a radiation environment of galactic cosmic rays in interplanetary space during solar minimum and again during solar flare. CRÈME-MC gives the omnidirectional flux in terms of particles/m^2-s-sr-MeV/nucleon. This will be denoted as h^*. The desired units of flux are particles/ cm^2 -day-MeV, which is calculated by $h_{U,OMNI}(\frac{E_{T,i}}{m}) = \frac{108.6}{m} \times h^*$. Finally, the stopping rate for the ion is calculated by $s_i = \rho \times L_i(E_{T,i}) \times h_{U,OMNI}(\frac{E_{T,i}}{m})$, where ρ is the density of silicon, 2.33 g/cm^3. Multiply this by 10^3 to get the desired units for s_i of particles/cm^3-day.

The tables of the stopping rates for ions hydrogen through uranium are included in the Appendix: The Stopping Rates.

Laser LET

The laser generation rate is given by

$$G(r,z,t) = \propto \frac{2TE_0}{E_\gamma \pi^{\frac{3}{2}} \omega_0^2 \tau} \frac{\omega_0^2}{\omega_{Si}(z)^2} e^{-\frac{2r^2}{\omega_{Si}(z)^2}} e^{-\propto z} e^{-\frac{t^2}{\tau^2}}$$

where $\omega_{Si}(z) = \omega_0 \sqrt{1+(\frac{z}{z_{sc}})^2}$, α = optical absorption of semiconductor, T = energy coefficient of surface of semiconductor, E_0 = energy of laser pulse, E_γ = energy of photon, ω_0 = laser beam waist, τ = laser pulse length, and z_{sc} = confocal length [6]. The equivalent laser LET is given by

$$LET = \frac{E_p}{d} \int_0^\infty \int_0^d \int_{-\infty}^\infty G(r,z,t) 2\pi r dr dz dt$$

where E_p is the pair generation energy [6]. Approximating $\omega_{Si}(z) \approx \omega_0$ and plugging in the generation equation,

$$LET \approx \frac{E_p}{d} \int_{r=0}^{\infty} \int_{z=0}^{d} \int_{t=-\infty}^{\infty} \alpha \frac{2TE_0}{E_\gamma \pi^{\frac{3}{2}} \omega_0^2 \tau} e^{-\frac{2r^2}{\omega_0^2}} e^{-\alpha z} e^{-\frac{t^2}{\tau^2}} 2\pi r\, dr\, dz\, dt$$

Integrating over r, z, and t,

$$LET \approx \frac{E_p}{d} \frac{2TE_o}{E_\gamma} (1 - e^{-\alpha d})$$

Plugging in the values for JPL's laser facility and dividing by the density of silicon,

$$LET = \frac{3.6\ MeV}{d} \frac{2E_0}{1.55\ MeV \times 2.33 \frac{g}{cm^3}} (1 - e^{-\frac{10^3 d}{cm}})$$

in units of MeV-cm^2/mg. The graph generated in MATLAB for device sensitivities *d* of 1 µm, 5 µm, 10 µm, and 20 µm of laser LET versus laser energy is shown in Figure 1. The laser energy depends on the laser's wavelength and pulse length.

Laser LET vs. Energy

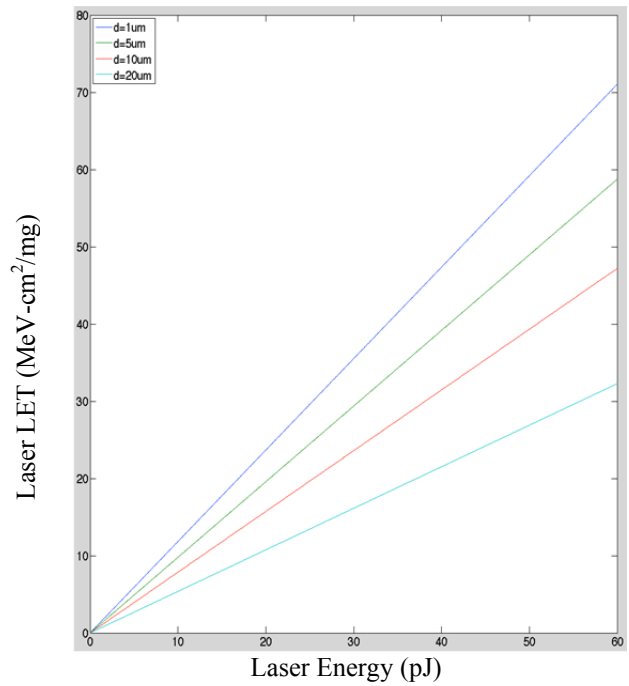

Figure 1. MATLAB plot of equivalent laser LET as a function of laser energy for certain device sensitivities.

IV. Results

The stopping rates per unit volume for ions hydrogen through uranium were calculated and are shown in the tables in the Appendix. A few ions have stopping rates of 0 because they are essentially non-existent for that radiation environment and are not included in the Crème-MC software.

For almost all ions, shielding was effective in lowering the stopping rate. Generally, the stopping rates for 250 mils of aluminum shielding were less than the stopping rates for 100 mils of shielding. While this may seem intuitive, shielding is not always effective at lowering SEE rates and can even increase the rates in certain cases.

The graph of laser LET vs. laser energy, shown in Figure 1, is an effective aid for using laser testing. It is easy to determine the necessary laser energy for the desired LET for a particular device sensitivity by looking at the graph. It is then simple to tune the laser to achieve this energy and accurately induce SEEs in integrated circuits. The graph shows that as device sensitivity depth increases, the average LET for a certain energy decreases, as is expected.

V. Conclusions

Overall, software was able to improve SEE testing at no additional cost. SRIM and Crème-MC were used to calculating the stopping rates for 92 different ions in four radiation environments. These reference tables will be extremely helpful in calculating much more precise SEGR rates than previous rate calculation methods. Additionally, the rate calculation that uses the stopping rate is not limited to SEGR; it can be applied to other SEEs that also require the use of a non-variable LET throughout the ion track. MATLAB was used to generate a graph of the equivalent laser LET versus laser energy. This graph will further make laser testing at JPL a valuable, affordable supplement to heavy ion testing.

VI. Acknowledgments

I would like to thank my mentor, Steven McClure, and co-mentor, Greg Allen, for the time they have spent working with me this summer, as well as Larry Edmonds and Dr. Philippe Adell for giving me the background knowledge and tools necessary to carry out my research. I would also like to thank my sponsor, NASA Space Grant, the Europa Habitability Mission team, the Jet Propulsion Laboratory, and the California Institute of Technology.

VII. References

[1] M. Baze, "Single Event Effects in Digital and Linear ICs," NSREC Short Course Notebook, Session III, July 2011.

[2] J. O. Bennett, and S. Shostale, "Life on Jovian Moons," *Life in the Universe,* Benjamin Cummings, San Francisco, 2011.

[3] L. D. Edmonds, C. E. Barnes, and L. Z. Scheick, "Basic Radiation Effects and Environmental Measures," *An Introduction to Space Radiation Effects on Microelectronics,* Jet Propulsion Laboratory, pp. 11-27, May 2000.

[4] T. R. Oldham, "Basic Mechanisms of TID and DDD Response in MOS and Bipolar Microelectronics," NSREC Short Course Notebook, Session II, July 2011.

[5] L. D. Edmonds, and L. Z. Scheick, "Effect of Shielding on Single-Event Rates in Devices that are Sensitive to Particle Range," NSREC Paper PI-8L, 2010.

[6] V. Pouget, H. Lapuyade, P. Fouillat, D. Lewis, S. Buchner, "Theoretical Investigation of an Equivalent Laser LET" *Microelectronics Reliability 41*, pp. 1513-1518, 2001.

[7] Software available at www.srim.org.

[8] Algorithms and documentation available at https://crème-mc.isde.vanderbilt.edu.

VIII. Appendix: The Stopping Rates

The tables of stopping rates for ions hydrogen to uranium for the four radiation environments are attached.

Stopping Rates of Ions for 100 mils aluminum shielding, IGCR											
						during solar minimum			during solar flare		
Atomic Number	Element	AMU	Shield Energy E (MeV)	E/m (MeV/nucleon)	LET (MeV-cm2/mg)	h* (1/m2-s-sr-MeV/nuc)	huomni (1/cm2-day-MeV)	Stopping Rate (1/cm3-day)	h* (1/m2-s-sr-MeV/nuc)	huomni (1/cm2-day-Mev)	Stopping Rate (1/cm3-day)
1	H	1.008	22.2	22.02380952	0.0187	0.37	39.86309524	1736.874923	540704	58254419.05	2538203292
2	He	4.003	88.8	22.18336248	0.0748	0.334	9.061304022	1579.24031	3519	95469.24806	16638762.43
3	Li	6.941	179	25.78879124	0.151	0.000389	0.006086356	2.141362784		0	0
4	Be	9.012	275	30.51486906	0.227	0.000102	0.001229161	0.650115607		0	0
5	B	10.81	384	35.51937841	0.321	0.000911	0.00915129	6.844524593		0	0
6	C	12.01	489	40.71268004	0.411	0.00454	0.041049371	39.31010954	23.26	210.3102156	201399.3718
7	N	14.01	628	44.83472549	0.529	0.00122	0.009458985	11.65886089	3.163	24.52358107	30227.03032
8	O	16	772	48.25301581	0.651	0.00562	0.038148134	57.86423449	14.8	100.4612788	152382.6816
9	F	19	946	49.79471523	0.804	9.81E-05	0.000560778	1.050516599	0.000404	0.002309422	4.326286504
10	Ne	20.18	1090	54.01387512	0.919	0.000905	0.004870317	10.42866399	1.31	7.049851338	15095.63517
11	Na	22.99	1300	56.54632449	1.11	0.000189	0.000892797	2.30904054	0.0814	0.384516746	994.4756612
12	Mg	24.31	1440	59.2470685	1.22	0.00117	0.005227813	14.86058182	0.854	3.81585682	10846.9546
13	Al	26.98	1680	62.26373138	1.46	0.000222	0.000893529	3.039607018	0.0557	0.224187236	762.6401392
14	Si	28.09	1830	65.15701773	1.58	0.000816	0.003155223	11.61563885	0.922	3.565092929	13124.53311
15	P	30.97	2070	66.83024472	1.8	2.72E-05	9.53677E-05	0.39997225	0.000491	0.001721528	7.220087312
16	S	32.07	2270	70.7937003	1.98	0.00013	0.000440293	2.031248439	0.174	0.589315453	2718.747911
17	Cl	35.45	2500	70.51589428	2.18	2.09E-05	6.40211E-05	0.325188767	0.000253	0.000774992	3.9364956
18	Ar	39.95	2860	71.59307099	2.51	3.92E-05	0.000106567	0.623233075	0.00242	0.006578853	38.47510312
19	K	39.1	2940	75.19566218	2.56	4.47E-05	0.00012416	0.740591448	0.000401	0.001113832	6.643784574
20	Ca	40.08	3160	78.84624981	2.76	0.000164	0.000444393	2.857805288	0.0539	0.146053695	939.2421037
21	Sc	44.96	3500	77.85390159	3.05	3.02E-05	0.000072954	0.518447597	0.000119	0.000287468	2.042889539
22	Ti	47.87	3780	78.96880941	3.31	0.00011	0.000249567	1.924731773	0.00148	0.003357804	25.89639113
23	V	50.94	4070	79.8947823	3.59	6.58E-05	0.000140275	1.173356806	0.000117	0.000249425	2.086363926
24	Cr	52	4310	82.89099161	3.81	0.000124	0.000258989	2.299124408	0.0049	0.010234249	90.85249677
25	Mn	54.94	4590	83.54872766	4.07	7.93E-05	0.000156758	1.486553343	0.00158	0.003123303	29.61859119
26	Fe	55.85	4830	86.48939028	4.29	0.000641	0.001246532	12.45996357	0.27	0.525060435	5248.346591
27	Co	58.93	5140	87.21768788	4.57	2.74E-06	5.04919E-06	0.053764296	0.00253	0.00466221	49.64367434
28	Ni	58.69	5340	90.98188881	4.76	2.92E-05	5.40289E-05	0.599224059	0.00524	0.009695603	107.5319887
29	Cu	63.55	5730	90.17089982	5.13	4.43E-07	7.57086E-07	0.009049376	5.21E-05	8.90388E-05	1.064271951
30	Zn	65.38	6000	91.77118385	5.36	5.76E-07	9.5677E-07	0.011948905	0.000119	0.000197666	2.468610552
31	Ga	69.72	6410	91.93522941	5.74	4.26E-08	6.63534E-08	0.000887424	7.76E-06	1.20869E-05	0.161652823
32	Ge	72.63	6820	93.90059204	6.13	9.25E-08	1.38311E-07	0.001975477	1.80E-05	2.69145E-05	0.384417086
33	As	74.92	7130	95.16563893	6.38	5.90E-09	8.55209E-09	0.00012713	1.03E-06	1.49299E-06	0.022193934
34	Se	78.96	7530	95.36474164	6.82	3.45E-08	4.74506E-08	0.000754019	1.01E-05	1.38913E-05	0.220741686
35	Br	79.9	7740	96.86623949	7.01	6.47E-09	8.79358E-09	0.000143628	1.27E-07	1.7261E-07	0.002819285
36	Kr	83.8	8250	98.45103702	7.5	1.81E-08	2.34571E-08	0.000409913	6.00E-06	7.77584E-06	0.135882837
37	Rb	85.47	8510	99.56942949	7.75	5.92E-09	7.52225E-09	0.000135833	8.60E-07	1.09276E-06	0.019732511
38	Sr	87.62	8890	101.4608537	8.08	1.96E-08	2.42931E-08	0.000457351	2.66E-06	3.29692E-06	0.062069107
39	Y	88.91	9210	103.5925584	8.38	4.42E-09	5.3991E-09	0.00010542	4.96E-07	6.05871E-07	0.011829881
40	Zr	91.22	9550	104.687363	8.72	1.09E-08	1.29762E-08	0.000263645	1.17E-06	1.39286E-06	0.028299514
41	Nb	92.91	9900	106.559318	9.04	1.99E-09	2.32616E-09	4.89963E-05	8.92E-06	1.04268E-05	0.21962171
42	Mo	95.96	10500	109.4205919	9.54	5.59E-03	0.006326323	140.6227833	4.01E-07	4.5382E-07	0.010087609
43	Tc	98	10700	109.1836735	9.79	6.56E-10	7.26955E-10	1.65824E-05		0	0
44	Ru	101.1	11200	110.8142871	10.2	2.15E-09	2.31018E-09	5.49038E-05	1.75E-07	1.88038E-07	0.004468911
45	Rh	102.9	11600	112.7242338	10.6	1.11E-09	1.17142E-09	2.89317E-05	3.56E-08	3.75698E-08	0.000927899
46	Pd	106.4	11900	111.8210863	11	3.19E-09	3.25535E-09	8.34345E-05	1.12E-07	1.14294E-07	0.002929363
47	Ag	107.9	12300	114.0282568	11.3	1.05E-09	1.05713E-09	2.78331E-05	3.44E-08	3.46334E-08	0.000911864
48	Cd	112.4	12800	113.8678599	11.9	2.79E-09	2.69541E-09	7.47357E-05	1.21E-07	1.16898E-07	0.003241226
49	In	114.8	13200	114.9645526	12.2	6.15E-10	5.81695E-10	1.65352E-05	1.50E-08	1.41877E-08	0.000403299
50	Sn	118.7	13800	116.2496841	12.7	3.29E-09	3.00981E-09	8.90632E-05	3.20E-07	2.92747E-07	0.008662677
51	Sb	121.8	14100	115.8015769	13.1	6.92E-10	6.17208E-10	0.000018839	2.28E-08	2.03357E-08	0.000620708
52	Te	127.6	14900	116.7711599	13.8	3.99E-09	3.39588E-09	0.000109191	4.70E-07	4.00016E-07	0.012862104
53	I	126.9	15100	118.9875812	14	7.74E-10	6.62362E-10	2.16063E-05	8.85E-08	7.57352E-08	0.002470482
54	Xe	131.3	15700	119.579871	14.5	1.90E-09	1.5716E-09	5.30965E-05	3.89E-07	3.21764E-07	0.010870807
55	Cs	132.9	16100	121.1391596	15	4.59E-10	3.7506E-10	1.31084E-05	2.75E-08	2.24709E-08	0.000785359
56	Ba	137.3	16400	119.4229831	15.3	4.72E-09	3.73264E-09	0.000133065	2.90E-08	2.29336E-08	0.000817559
57	La	138.9	16800	120.9459703	15.8	4.23E-10	3.30714E-10	1.21749E-05	2.75E-08	2.15003E-08	0.000791512
58	Ce	140.1	17100	122.0417368	16	1.27E-09	9.84342E-10	3.66963E-05	6.67E-08	5.16973E-08	0.001927276
59	Pr	140.9	17400	123.484827	16.3	3.05E-09	2.35068E-09	8.92766E-05	1.02E-08	7.8613E-09	0.000298564
60	Nd	144.2	18100	125.4835623	16.9	1.14E-09	8.58308E-10	3.37976E-05	4.81E-08	3.62146E-08	0.001426021
61	Pm	145	18300	126.2068966	17.2	1.35E-10	1.0111E-10	4.0521E-06		0	0

62	Sm	150.4	18900	125.698324	17.8	1.28E-09	9.24501E-10	3.83428E-05	1.20E-08	8.6672E-09	0.000359463
63	Eu	152	19400	127.6618146	18.3	2.21E-10	1.57936E-10	6.73424E-06	4.53E-09	3.23733E-09	0.000138037
64	Gd	157.3	19800	125.9141494	18.7	9.95E-10	6.87167E-10	2.99406E-05	2.36E-08	1.62986E-08	0.000710148
65	Tb	158.9	19900	125.216297	18.8	2.48E-10	1.69469E-10	7.4234E-06	3.63E-09	2.48053E-09	0.000108657
66	Dy	162.5	20800	128	19.8	9.98E-10	6.66971E-10	0.00003077	2.24E-08	1.49701E-08	0.00069063
67	Ho	164.9	21700	131.5709695	20.6	3.79E-10	2.49557E-10	1.19782E-05	4.13E-09	2.71944E-09	0.000130528
68	Er	167.3	21500	128.5431576	20.4	6.28E-10	4.07756E-10	1.93814E-05	1.11E-08	7.20715E-09	0.00034257
69	Tm	168.9	21900	129.6364261	20.9	1.29E-10	8.29282E-11	4.03836E-06	2.12E-09	1.36285E-09	6.63668E-05
70	Yb	173.1	22300	128.8615114	21.2	6.35E-10	3.98494E-10	0.000019684	9.82E-09	6.16254E-09	0.000304405
71	Lu	175	22700	129.7387507	21.8	9.29E-11	5.7662E-11	2.92888E-06	2.12E-09	1.31586E-09	6.68378E-05
72	Hf	178.5	23400	131.0997815	22.5	5.79E-10	3.52285E-10	1.84686E-05	8.34E-09	5.07437E-09	0.000266024
73	Ta	180.9	23900	132.0821451	23	5.22E-10	3.1329E-10	1.67892E-05	9.18E-10	5.50958E-10	2.95259E-05
74	W	183.8	24500	133.2680592	23.6	5.81E-10	3.43215E-10	1.88727E-05	9.93E-09	5.86596E-09	0.000322557
75	Re	186.2	25000	134.2591847	24.2	2.01E-10	1.17228E-10	0.00000661	1.95E-09	1.13728E-09	6.41268E-05
76	Os	190.2	25600	134.5739368	25	8.61E-10	4.91534E-10	2.86319E-05	2.90E-08	1.65557E-08	0.000964372
77	Ir	192.2	26100	135.7840358	25.5	5.67E-10	3.20347E-10	1.90334E-05	2.82E-08	1.59326E-08	0.000946636
78	Pt	195.1	26700	136.8641201	26.1	1.08E-09	6.01218E-10	3.65619E-05	5.53E-08	3.07846E-08	0.001872103
79	Au	197	27000	137.0788	26.5	2.01E-10	1.10824E-10	6.84281E-06	9.17E-09	5.05598E-09	0.000312182
80	Hg	200.6	27700	138.0926268	27.2	3.53E-10	1.91115E-10	1.21121E-05	8.97E-09	4.85638E-09	0.000307778
81	Tl	204.4	28200	137.9762505	27.8	1.08E-10	5.73864E-11	3.71715E-06	8.00E-09	4.25084E-09	0.000275344
82	Pb	207.2	28400	137.0656371	27.8	1.01E-09	5.29373E-10	3.42896E-05	9.16E-08	4.80104E-08	0.003109827
83	Bi	209	29100	139.2477749	28.9	5.26E-11	2.73345E-11	1.84062E-06	5.26E-09	2.73345E-09	0.000184062
84	Po	209	29500	141.1483254	29.2		0	0		0	0
85	At	210	29800	141.9047619	29.6		0	0		0	0
86	Rn	222	30700	138.2882883	30.6		0	0		0	0
87	Fr	223	31000	139.0134529	31		0	0		0	0
88	Ra	226	31500	139.380531	31.4		0	0		0	0
89	Ac	227	31800	140.0881057	31.6		0	0		0	0
90	Th	232	32200	138.7703738	32	5.84E-11	2.73328E-11	2.03793E-06	1.77E-09	8.28407E-10	6.17661E-05
91	Pa	231	32300	139.805052	31.9		0	0		0	0
92	U	238	34400	144.5202055	33.7	3.54E-11	1.61511E-11	1.2682E-06	9.46E-10	4.3161E-10	3.38904E-05

Stopping Rates of Ions for 250 mils aluminum shielding, IGCR											
						during solar minimum			during solar flare		
Atomic Number	Element	AMU	Shield Energy E (MeV)	E/m (MeV/nucleon)	LET (MeV-cm2/mg)	h* (1/m2-s-sr-MeV/nuc)	huomni (1/cm2-day-MeV)	Stopping Rate (1/cm3-day)	h* (1/m2-s-sr-MeV/nuc)	huomni (1/cm2-day-Mev)	Stopping Rate (1/cm3-day)
1	H	1.008	37.2	36.9047619	0.0125	0.61	65.7202381	1914.101935	168000	18100000	527162500
2	He	4.003	148.5	37.09717712	0.0498	0.289	7.840469648	909.7610551	507	13754.73395	1596016.799
3	Li	6.941	300	43.22143783	0.101	0.000585	0.009153004	2.153976405		0	0
4	Be	9.012	456.2	50.6213937	0.152	0.00019	0.002289614	0.81088964		0	0
5	B	10.811	639.7	59.1712145	0.215	0.00142	0.01426436	7.145731329		0	0
6	C	12.011	816.9	68.01265507	0.276	0.00623	0.056329864	36.22460913	0.602	5.443110482	3500.355489
7	N	14.007	1050	74.96251874	0.355	0.00155	0.012017563	9.940326944	0.107	0.829599486	686.2032148
8	O	15.999	1293	80.8175511	0.437	0.00651	0.044189387	44.99407557	0.668	4.534333396	4616.903607
9	F	18.998	1588	83.58774608	0.539	1.39E-04	0.000794578	0.997887146	2.68E-05	0.000153199	0.192398385
10	Ne	20.18	1824	90.38652131	0.62	0.0011	0.005919722	8.55163112	0.0933	0.502100099	725.3338032
11	Na	22.99	2185	95.04132231	0.749	0.000241	0.001138434	1.986761041	0.00632	0.029854371	52.10095345
12	Mg	24.305	2414	99.32112734	0.827	0.00146	0.006523596	12.57038231	0.0633	0.282838099	545.0035616
13	Al	26.982	2851	105.6630346	0.989	0.000271	0.001090749	2.513490168	0.00444	0.01787058	41.18042933
14	Si	28.086	3097	110.2684612	1.07	0.000993	0.003839628	9.572577276	0.0744	0.287682119	717.2202914
15	P	30.974	3512	113.38542	1.21	3.77E-05	0.000132182	0.372662054	4.25E-05	0.000149012	0.420109742
16	S	32.065	3861	120.4116638	1.35	0.000167	0.000565607	1.779117951	0.0145	0.049109621	154.4743131
17	Cl	35.453	4248	119.8206076	1.48	3.13E-05	9.58785E-05	0.330627375	2.54E-05	7.78055E-05	0.268304643
18	Ar	39.948	4873	121.9835787	1.7	5.88E-05	0.00015985	0.633165077	2.51E-04	0.000682352	2.7027965
19	K	39.098	4995	127.7558954	1.74	6.16E-05	0.000171102	0.693683181	4.34E-05	0.000120549	0.488731332
20	Ca	40.078	5375	134.1134787	1.88	0.000192	0.000520265	2.278970919	0.00478	0.012952443	56.73688016
21	Sc	44.956	5944	132.2181689	2.08	3.63E-05	8.76897E-05	0.424979561	1.22E-05	2.94715E-05	0.142830596
22	Ti	47.867	6439	134.5185618	2.25	0.00013	0.000294942	1.546234671	0.000174	0.000394769	2.069575637
23	V	50.942	6961	136.645597	2.44	7.25E-05	0.000154558	0.878693852	1.56E-05	3.32566E-05	0.189070677
24	Cr	51.996	7365	141.6455112	2.6	0.000138	0.00028823	1.746096515	5.65E-04	0.001180072	7.148873413
25	Mn	54.938	7865	143.1613819	2.77	8.54E-05	0.000168816	1.08955847	1.87E-09	3.69657E-09	2.3858E-05
26	Fe	55.845	8278	148.2317128	2.93	0.000725	0.001409885	9.625140505	0.0301	0.058534515	399.6092817
27	Co	58.933	8815	149.5766379	3.12	3.60E-06	6.63397E-06	0.048226339	3.82E-04	0.000703938	5.11735038
28	Ni	58.693	9175	156.3218782	3.26	3.36E-05	6.21703E-05	0.472232981	8.19E-04	0.0015154	11.51067892
29	Cu	63.546	9868	155.2890819	3.51	4.94E-07	8.44245E-07	0.00690449	8.03E-06	1.37233E-05	0.112232901
30	Zn	65.38	10330	157.9993882	3.68	6.40E-07	1.06308E-06	0.009115251	1.94E-05	3.22245E-05	0.27630604
31	Ga	69.723	11040	158.3408631	3.93	4.73E-08	7.36741E-08	0.000674626	1.21E-06	1.88469E-06	0.017257886
32	Ge	72.63	11760	161.9165634	4.2	1.02E-07	1.52515E-07	0.001492517	2.85E-06	4.26146E-06	0.041702669
33	As	74.922	12260	163.636849	4.38	6.48E-09	9.39281E-09	9.58574E-05	1.66E-07	2.40618E-07	0.002455605
34	Se	78.96	13040	165.1469098	4.66	3.79E-08	5.21269E-08	0.000565983	1.62E-06	2.22812E-06	0.024192432
35	Br	79.904	13390	167.5760913	4.81	7.06E-09	9.59546E-09	0.000107539	2.06E-07	2.79981E-07	0.003137831
36	Kr	83.798	14320	170.8871333	5.17	1.97E-08	2.55307E-08	0.000307545	9.77E-07	1.26617E-06	0.015252365
37	Rb	85.468	14770	172.8132166	5.33	6.41E-09	8.14487E-09	0.00010115	1.47E-07	1.86786E-07	0.002319673
38	Sr	87.62	15430	176.1013467	5.57	2.11E-08	2.61522E-08	0.000339406	4.48E-07	5.5527E-07	0.007206356
39	Y	88.906	16000	179.9653567	5.78	4.73E-09	5.77777E-09	7.78115E-05	8.43E-08	1.02974E-07	0.001386788
40	Zr	91.224	16620	182.1888977	6.02	1.16E-08	1.38095E-08	0.000193701	2.03E-07	2.41667E-07	0.003389762
41	Nb	92.906	17240	185.5639033	6.26	2.11E-09	2.46643E-09	3.59748E-05	1.54E-08	1.80014E-08	0.000262565
42	Mo	95.96	18220	189.8707795	6.63	5.88E-09	6.65452E-09	0.000102798	7.22E-08	8.17103E-08	0.001262252
43	Tc	98	18649	190.2959184	6.81	6.89E-10	7.63524E-10	1.21151E-05		0	0
44	Ru	101.07	19520	193.1334719	7.13	2.25E-09	2.41763E-09	4.01639E-05	3.09E-08	3.32021E-08	0.000551584
45	Rh	102.91	20230	196.5871766	7.4	1.16E-09	1.22419E-09	2.11074E-05	6.54E-09	6.90187E-09	0.000119002
46	Pd	106.42	20860	196.0157865	7.66	3.33E-09	3.39821E-09	6.06507E-05	2.06E-08	2.1022E-08	0.000375196
47	Ag	107.87	21500	199.3176846	7.9	1.08E-09	1.08733E-09	2.00145E-05	6.29E-09	6.33268E-09	0.000116566
48	Cd	112.41	22520	200.336266	8.25	2.89E-09	2.79202E-09	5.36696E-05	2.17E-08	2.09643E-08	0.000402987
49	In	114.82	23140	201.5363445	8.52	6.36E-10	6.01557E-10	1.19419E-05	2.72E-09	2.5727E-09	5.10722E-05
50	Sn	118.71	24100	203.0157527	8.89	3.39E-09	3.10129E-09	6.42392E-05	5.99E-08	5.47986E-08	0.001135081
51	Sb	121.76	24800	203.6793693	9.15	7.14E-10	6.3683E-10	1.35769E-05	4.13E-09	3.68362E-09	7.8533E-05
52	Te	127.6	26100	204.5454545	9.66	4.11E-09	3.49801E-09	7.87325E-05	9.15E-08	7.78754E-08	0.001752804
53	I	126.9	26480	208.6616655	9.81	7.91E-10	6.7691E-10	1.54723E-05	1.67E-08	1.42913E-08	0.00032666
54	Xe	131.29	27550	209.8360156	10.2	1.94E-09	1.60469E-09	3.8137E-05	7.34E-08	6.07134E-08	0.001442914

						during solar minimum			during solar flare		
Atomic Number	Element	AMU	Shield Energy E (MeV)	E/m (MeV/nucleon)	LET (MeV-cm2/mg)	h* (1/m2-s-sr-MeV/nuc)	huomni (1/cm2-day-MeV)	Stopping Rate (1/cm3-day)	h* (1/m2-s-sr-MeV/nuc)	huomni (1/cm2-day-Mev)	Stopping Rate (1/cm3-day)
55	Cs	132.91	28320	213.0845341	10.5	4.67E-10	3.81597E-10	9.33578E-06	5.19E-09	4.24088E-09	0.000103753
56	Ba	137.33	28920	210.592236	10.8	4.82E-09	3.81172E-09	9.59181E-05	5.37E-08	4.24667E-08	0.001068631
57	La	138.91	29700	213.8151974	11	4.31E-10	3.36968E-10	8.6365E-06	5.15E-09	4.02642E-09	0.000103197
58	Ce	140.12	30140	215.1074824	11.2	1.29E-09	9.99843E-10	2.60919E-05	1.26E-08	9.76591E-09	0.000254851
59	Pr	140.91	30750	218.227496	11.5	3.08E-10	2.3738E-10	6.36061E-06	1.94E-09	1.49519E-09	4.00636E-05
60	Nd	144.24	31960	221.5720803	11.9	1.14E-09	8.58308E-10	2.37983E-05	9.29E-09	6.99445E-09	0.000193935
61	Pm	145	32440	223.7241379	12.1	1.35E-10	1.0111E-10	2.8506E-06		0	0
62	Sm	150.36	33440	222.3995744	12.5	1.29E-09	9.31724E-10	2.71365E-05	2.31E-09	1.66844E-09	4.85932E-05
63	Eu	151.96	34380	226.2377932	12.9	2.20E-10	1.57221E-10	4.72561E-06	8.75E-10	6.25313E-10	1.8795E-05
64	Gd	157.25	35100	223.2114467	13.2	9.99E-10	6.89929E-10	2.12195E-05	4.55E-09	3.14232E-09	9.66452E-05
65	Tb	158.93	35340	222.369042	13.3	2.50E-10	1.70835E-10	5.29402E-06	6.90E-10	4.71505E-10	1.46115E-05
66	Dy	162.5	37050	228	14	9.94E-10	6.64298E-10	2.16694E-05	4.28E-09	2.86036E-09	9.33048E-05
67	Ho	164.93	38560	233.7961559	14.6	3.75E-10	2.46923E-10	8.39982E-06	7.96E-10	5.24135E-10	1.783E-05
68	Er	167.26	38220	228.507883	14.5	6.26E-10	4.06457E-10	1.37322E-05	2.13E-09	1.38299E-09	4.67244E-05
69	Tm	168.93	39000	230.8593889	14.8	1.28E-10	8.22854E-11	2.83753E-06	4.13E-10	2.65499E-10	9.15547E-06
70	Yb	173.05	39720	229.5237325	15.1	6.32E-10	3.96611E-10	1.3954E-05	1.90E-09	1.19234E-09	4.19503E-05
71	Lu	174.97	40630	232.2152177	15.5	9.21E-11	5.71654E-11	2.06453E-06	4.06E-10	2.52E-10	9.10096E-06
72	Hf	178.49	41880	234.6349936	16	5.73E-10	3.48635E-10	1.29971E-05	1.58E-09	9.61331E-10	3.58384E-05
73	Ta	180.95	42800	236.5320424	16.4	5.15E-11	3.09089E-11	1.18109E-06	1.73E-10	1.0383E-10	3.96755E-06
74	W	183.84	43920	238.9033943	16.8	5.71E-10	3.37307E-10	1.32036E-05	1.85E-09	1.09285E-09	4.27786E-05
75	Re	186.21	44950	241.398014	17.3	1.97E-10	1.14895E-10	4.63129E-06	3.67E-10	2.14042E-10	8.62784E-06
76	Os	190.23	46190	242.8113336	17.8	8.43E-10	4.81258E-10	1.99597E-05	5.35E-09	3.05425E-09	0.000126672
77	Ir	192.22	47080	244.9315097	18.2	5.54E-10	3.13002E-10	1.32732E-05	5.23E-09	2.95488E-09	0.000125305
78	Pt	195.08	48240	247.2780956	18.7	1.05E-09	5.84517E-10	2.5468E-05	1.00E-08	5.56683E-09	0.000242552
79	Au	196.97	48840	247.9603182	19	1.96E-10	1.08067E-10	4.78412E-06	1.67E-09	9.20774E-10	4.07626E-05
80	Hg	200.59	50200	250.2617279	19.5	3.42E-10	1.8516E-10	8.41273E-06	1.64E-09	8.87901E-10	4.03418E-05
81	Tl	204.38	51190	250.461144	20	1.05E-10	5.57923E-11	2.59992E-06	1.47E-09	7.81092E-10	3.63989E-05
82	Pb	207.2	51340	247.7799228	20	9.80E-10	5.13649E-10	2.3936E-05	1.69E-08	8.85782E-09	0.000412774
83	Bi	208.98	53020	253.7084889	20.8	5.08E-11	2.63991E-11	1.27941E-06	9.45E-10	4.91085E-10	2.38E-05
84	Po	209	53710	256.9856459	21.1		0	0		0	0
85	At	210	54320	258.6666667	21.4		0	0		0	0
86	Rn	222	56020	252.3423423	22		0	0		0	0
87	Fr	223	56630	253.9461883	22.3		0	0		0	0
88	Ra	226	57440	254.159292	22.6		0	0		0	0
89	Ac	227	57980	255.4185022	22.8		0	0		0	0
90	Th	232.04	58720	253.0619985	23	5.64E-11	2.63967E-11	1.4146E-06	3.17E-10	1.48364E-10	7.95085E-06
91	Pa	231.04	58720	254.1595249	22.9		0	0		0	0
92	U	238.03	62220	261.3967206	24.3	3.39E-11	1.54668E-11	8.75713E-07	1.74E-10	7.9387E-11	4.49481E-06